

## Analysis of Electrical Properties of Narrow Channel SOI MOSFETs

Prashant Mani<sup>1</sup>, Pankaj Singh<sup>2</sup>, Anand Pandey<sup>3</sup>, Nishant Srivastav<sup>4</sup>, Vipin Kr.Yadav<sup>5</sup>

<sup>1</sup>Associate Professor, <sup>2,3,4,5</sup>Assistant Professor  
 SRMIST, NCR Campus, Ghaziabad (U.P.) India 201204

ORCID: 0000-0001-7473-6684 (Prashant Mani), 0000-0002-7880-4901(Pankaj Singh)  
 0000-0002-9834-3428(Anand Pandey), 0000-0002-6556-7580 (Nishant Srivastava)  
 0000-0002-0924-6141 (Vipin Kumar Yadav)

### Abstract

This paper presents the analysis of electrical characteristics of nano structured Fully Depleted narrow channel SOIMOSFET. The mathematical solution of 3D Poisson's equation used separation of variable technique; the surface potential is calculated. The boundary conditions of proposed device are considered in calculations. The impact of narrow channel effect and short channel effect in proposed device analysed. The narrow channel width effect on the threshold voltage is also investigated for thin film Fully Depleted(FD)narrow channel SOI MOSFET.

**Keywords:** Channel length<sup>1</sup>; Threshold voltage<sup>2</sup>; 3D modelling<sup>3</sup>.

### I. INTRODUCTION

The ongoing downscaling in physical size of traditional complementary MOS (CMOS) has been foiled by the increasing deleterious existence of the short-channel effects (SCEs). As the semiconductor MOSFETs starts to enter in to the deep sub-micro-meter regime, the short-channel effects (SCEs) event will take on a more prominent role in influencing their performance. Suppression of the SCEs has become essential for increasing the performance of MOSFETs. Due to above most of work on reducing the SCE is currently being carried out by researchers. In some cases, focus is now on development of multiple-gate and multi material structure of MOSFETs because of their abrupt sub-threshold slope and lowered body-effect coefficient. The self-heating effect [3]. Further an improved complete shrunk channel MOSFET I-V model related to circuit simulation developed. This unified model is applicable for Fully Depleted, Partially Depleted, and mixed-mode SOI MOSFET's [4]. The various methods to solve 1D, 2D analysis of SOI MOSFET were very interesting areas for work [5-11]. In present model, 3D Poisson's equation is solved with various boundary conditions using separation of variable method.

### II. MODEL FORMULATION

Figure 1 shows the cross-sectional view (x-y) of the fully depleted SOI MOSFET. At  $y=0$ , the source- channel junction is located and the channel drain junction is located at  $y= L_{eff}$ . This implies the  $y$  varies from 0 to  $L_{eff}$ . Here,  $L_{eff}$  is the effective channel length of the device. Si-SiO<sub>2</sub> interface is located at  $x=0$  and  $x= t_s$ . The term  $t_s$  represent the thickness of the Si film,  $t_{oxf}$  and  $t_{oxb}$  represents the front gate oxide

thickness and back gateoxide thickness of the proposed device respectively.  $V_{gf}$  and  $V_{gb}$  are the potential applied at the front gate and the back gate respectively.

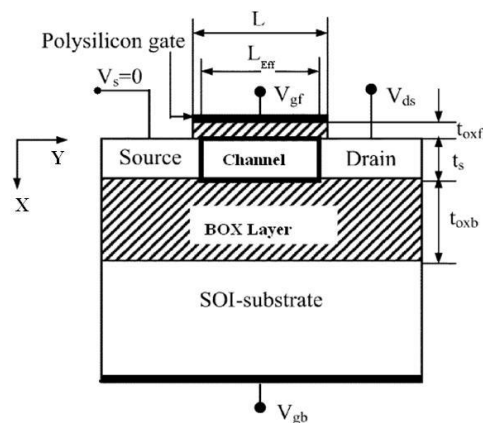


Fig 1. Cross-sectional view(x-y)

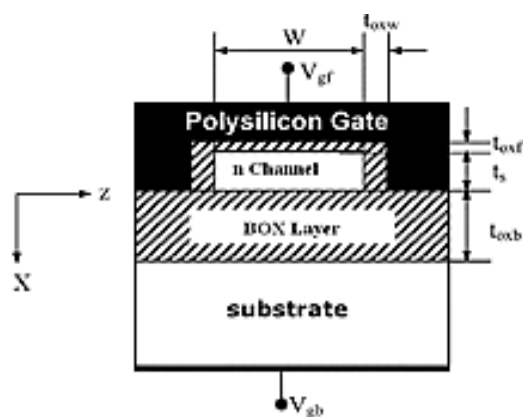


Fig 2. Cross-sectional view(x-z)

Cross-sectional view (x-z) of the fully depleted SOI MOSFET is shown in the figure 2. This device has the channel width of  $W$ .  $t_{oxw}$  is the thickness of the side wall. Side wall interface junction is located at  $z=0$  and  $z=W$ .

### III. SURFACE POTENTIAL FORMULATION

To analyse the proposed structure given above, solution of Poisson's equation and also the current continuity equation is required. However, in case of subthreshold calculation, the currents are less and hence alone Poisson's equation will provide the required result.

The Poisson's equation is given by,

$$\frac{\partial^2 \varphi(x,y,z)}{\partial x^2} + \frac{\partial^2 \varphi(x,y,z)}{\partial y^2} + \frac{\partial^2 \varphi(x,y,z)}{\partial z^2} = \frac{qN_A}{\epsilon_{si}}$$

Here,  $N_A$  represents the doping concentration and  $\varphi(x,y,z)$  is the surface potential at  $(x,y,z)$  point. The required boundary conditions to solve the Poisson's equation are given by,

$$\varphi(0,y,z) - \frac{t_{oxf}}{\epsilon_{ox}} \epsilon_{si} \frac{\partial \varphi(x,y,z)}{\partial x} \Big|_{x=0} - Q_{it}^f = V_{gf} - V_{fb}^f$$

$$\varphi(t_s,y,z) + \frac{t_{oxb}}{\epsilon_{ox}} \epsilon_{si} \frac{\partial \varphi(x,y,z)}{\partial x} \Big|_{x=t_s} + Q_{it}^b = V_{gf} - V_{fb}^b$$

$$\varphi(x,0,z) = V_{bi}$$

$$\varphi(x,L_{eff},z) = V_{bi} + V_{ds}$$

$$\varphi(x,y,0) - \frac{t_{oxw}}{\epsilon_{ox}} \epsilon_{si} \frac{\partial \varphi(x,y,z)}{\partial x} \Big|_{z=0} - Q_{it}^f = V_{gf} - V_{fb}^f$$

$$\varphi(x,y,w) + \frac{t_{oxw}}{\epsilon_{ox}} \epsilon_{si} \frac{\partial \varphi(x,y,z)}{\partial x} \Big|_{z=w} + Q_{it}^f = V_{gf} - V_{fb}^f$$

The above boundary conditions will be useful in finding the solution of the Poisson's equation of MOSFET. There are methods such as Green function technique which is used to solve the equation. However, we have applied the technique of variable separable to solve the 3d Poisson's equation.

Using the method, the solution is given by,

$$\frac{d^2 \varphi(x)}{dx^2} = \frac{qN_A x}{\epsilon_{si}}$$

$$\frac{d^2 \varphi'(x,y)}{dx^2} + \frac{d^2 \varphi'(x,y)}{dy^2} = 0$$

$$\frac{d^2 \varphi''(x,y,z)}{dx^2} + \frac{d^2 \varphi''(x,y,z)}{dy^2} + \frac{d^2 \varphi''(x,y,z)}{dz^2} = 0$$

The 1-D Poisson's Equation will provide the solution as  $\varphi(x)$  and the solution of 2-D and 3-D equation will be  $\varphi'(x,y)$  and  $\varphi''(x,y,z)$  respectively.

The solution of the 3D Poisson's equation will be the sum of all the Laplace equation, i.e.

$$\varphi(x,y,z) = \varphi(x) + \varphi'(x,y) + \varphi''(x,y,z)$$

### III.I. SOLUTION OF THE 1-D LAPLACE EQUATION

Solution of 1-D Laplace Equation is provided with the help of the boundary conditions given as,

$$\varphi(x) - \frac{t_{oxf}}{\epsilon_{ox}} \epsilon_{si} \frac{d\varphi(x)}{dx} \Big|_{x=0} - Q_{it}^f = V_{gf} - V_{fb}^f$$

$$\varphi(t_s) + \frac{t_{oxb}}{\epsilon_{ox}} \epsilon_{si} \frac{d\varphi(x)}{dx} \Big|_{x=t_s} + Q_{it}^b = V_{gf} - V_{fb}^b$$

After solving all the equations, the solution is given as,

$$\psi_1 = \psi_{sb} + E_{sb} \cdot (t_s - x) + \frac{q \cdot N_A}{2 \cdot \epsilon_{si}} (t_s - x)^2$$

### III.II. SOLUTION OF THE 2-D LAPLACE EQUATION

Using the boundary conditions, the equation solution is given as,

$$\varphi'(x,y) - \frac{t_{oxf}}{\epsilon_{ox}} \epsilon_{si} \frac{d\varphi'(x,y)}{dx} \Big|_{x=0} = 0$$

$$\varphi'(x,y) + \frac{t_{oxb}}{\epsilon_{ox}} \epsilon_{si} \frac{d\varphi'(x,y)}{dx} \Big|_{x=t_s} = 0$$

$$\varphi'(x,0) = V_{bi} - \varphi(x)$$

$$\varphi'(x,L_{eff}) = V_{bi} - \varphi(x) + V_{ds}$$

$$\psi_2 = \frac{1}{\sinh(\gamma_r \cdot L_{eff})} \cdot \left( (V_r \cdot \sinh(\gamma_r \cdot y) + V \cdot \sinh(\gamma_r \cdot (L_{eff} - y))) \cdot \left[ \sin(\gamma_r \cdot x) + \frac{\epsilon_{si}}{\epsilon_{ox}} \cdot t_{oxf} \cdot \gamma_r \cdot \cos(\gamma_r \cdot x) \right] \right)$$

Here  $V$  and  $V_r$  will be described as follows,

$$V := \frac{i_{dmm1} + \frac{\epsilon_{si}}{\epsilon_{ox}} \cdot t_{oxf} \cdot \gamma_r \cdot i_{dmm2}}{i_{dmm}}$$

and

$$V_r = V + \frac{V_{ds} \cdot \left( \frac{1}{\gamma_r} \cdot (1 - \cos(\gamma_r \cdot t_s)) + \frac{\epsilon_{si}}{\epsilon_{ox}} \cdot t_{oxf} \cdot \sin(\gamma_r \cdot t_s) \right)}{i_{dmm}}$$

the various terms used in equation as follows

$$i_{dmm} = \frac{1}{4 \cdot \gamma_r} \cdot (2 \cdot \beta_s \cdot t_s - \sin(2 \cdot \gamma_r \cdot t_s)) + \left( \frac{\epsilon_{si}}{\epsilon_{ox}} \cdot t_{oxf} \cdot \gamma_r \right)^2 \cdot \frac{1}{4 \cdot \gamma_r} \cdot$$

$$\left[ 2 \cdot \gamma_r \cdot t_s - \sin(2 \cdot \gamma_r \cdot t_s) \right] + \frac{\epsilon_{si} \cdot t_{oxf}}{2 \cdot \epsilon_{ox}} \cdot (1 - \cos(2 \cdot \gamma_r \cdot t_s))$$

$$i_{dmm1} = \frac{q \cdot N_A}{\epsilon_{si} \cdot \gamma_r^3} \cdot (1 - \cos(\gamma_r \cdot t_s)) + E_{sb} \cdot \frac{\sin(\gamma_r \cdot t_s)}{\gamma_r^2} + \left( V_{bi} - \psi_{sb} - E_{sb} \cdot t_s - \frac{q}{2 \cdot \epsilon_{si}} \cdot N_A \cdot t_s^2 \right)$$

$$\cdot \frac{1}{\gamma_r} - (V_{bi} - \psi_{sb}) \cdot \frac{\cos(\gamma_r \cdot t_s)}{\gamma_r}$$

$$i_{dmm2} = \frac{q \cdot 10^{18}}{\epsilon_{si} \cdot \gamma_r^3} \cdot \sin(\gamma_r \cdot t_s) + E_{sb} \cdot \frac{\cos(\gamma_r \cdot t_s)}{\gamma_r^2} - \left( E_{sb} + \frac{q \cdot N_A \cdot t_s}{\epsilon_{si}} \right) \cdot \frac{1}{\gamma_r^2} + (V_{bi} - \psi_{sb}) \cdot \frac{\sin(\gamma_r \cdot t_s)}{\gamma_r}$$

### III.III. SOLUTION OF THE 3-D LAPLACE EQUATION

The solution of the 3-D Laplace Equation is done with the help of the following boundary conditions,

$$\varphi''(x,y,z) - \frac{t_{oxf}}{\epsilon_{ox}} \epsilon_{si} \frac{\partial \varphi''(x,y,z)}{\partial x} \Big|_{x=0} = 0$$

$$\varphi''(x,y,z) + \frac{t_{oxb}}{\epsilon_{ox}} \epsilon_{si} \frac{\partial \varphi''(x,y,z)}{\partial x} \Big|_{x=t_s} = 0$$

$$\varphi''(x,0,z) = 0$$

$$\varphi''(x,L_{eff},z) = 0$$

$$\varphi''(x,y,0) - \frac{t_{oxw}}{\epsilon_{ox}} \epsilon_{si} \frac{\partial \varphi''(x,y,z)}{\partial x} \Big|_{z=0} - Q_{it}^f = V_{gf} - V_{fb}^f -$$

$$\varphi(x) - \varphi'(x,y)$$

$$\varphi''(x,y,w) + \frac{t_{oxw}}{\epsilon_{ox}} \epsilon_{si} \frac{\partial \varphi''(x,y,z)}{\partial x} \Big|_{z=w} + Q_{it}^f = V_{gf} - V_{fb}^f -$$

$$\varphi(x) - \varphi'(x,y)$$

After solving the above equations, the solution of the 3D Poisson's equation is given by,

$$\psi_v := M_{sr} \cdot (\sinh(\chi_{sr} \cdot W - z) + \sinh(\chi_{sr} \cdot z)) \cdot \frac{\sin(\alpha_s \cdot y - L_{eff})}{\cos(\alpha_s \cdot L_{eff})}$$

$$\cdot \left[ \sin(x \cdot \beta_r) + \frac{t_{oxf}}{\epsilon_{ox}} \cdot \epsilon_{si} \cdot \cos(\beta_r \cdot x) \right]$$

Here

$$i_{Dnum3d} := \frac{1}{4 \cdot \beta_r} \cdot (2 \cdot \beta_r \cdot t_s - \sin(2 \cdot \beta_r \cdot t_s)) + \left( \frac{\epsilon_{si}}{\epsilon_{ox}} \cdot t_{oxf} \cdot \beta_r \right) \cdot \frac{1}{4 \cdot \beta_r} \cdot [2 \cdot \beta_r \cdot t_s - \sin(2 \cdot \beta_r \cdot t_s)]$$

$$+ \left( \frac{\epsilon_{si} \cdot t_{oxf}}{2 \cdot \epsilon_{ox}} \right) \cdot [1 - \cos(2 \cdot \beta_r \cdot t_s)] \cdot \left[ \frac{1}{2 \cdot \cos(\alpha_s \cdot L_{eff})^2} \cdot \left( L_{eff} - \frac{\sin(2 \cdot \alpha_s \cdot L_{eff})}{2 \cdot \alpha_s} \right) \right]$$

$$i_{num3d} := \frac{q \cdot N_A}{\epsilon_{si} \cdot \beta_r^3} \cdot [1 - \cos(\beta_r \cdot t_s)] + E_{sb} \cdot \frac{\sin(\beta_r \cdot t_s)}{\beta_r^2} + [V_{gf} - V_{f0f} - \psi_{sb} - E_{sb} \cdot t_s -$$

$$\left( \frac{q}{2 \cdot \epsilon_{si}} \cdot N_A \cdot t_s^2 \right)] \cdot \frac{1}{\beta_r} - [V_{gf} - V_{f0f} - \psi_{sb}] \cdot \frac{\cos(\beta_r \cdot t_s)}{\beta_r^2}$$

$$i_2 := \frac{q \cdot N_A}{\epsilon_{si} \cdot \beta_r^3} \cdot \sin(\beta_r \cdot t_s) + E_{sb} \cdot \frac{\cos(\beta_r \cdot t_s)}{\beta_r^3} - E_{sb} - \frac{q \cdot N_A \cdot t_s}{\epsilon_{si}} \cdot \frac{1}{\beta_r^2} -$$

$$[V_{gf} - V_{f0f} - \psi_{sb}] \cdot \frac{\sin(\beta_r \cdot t_s)}{\beta_r^2}$$

$$i_3 := \frac{1}{4 \cdot \beta_r} \cdot (2 \cdot \beta_r \cdot t_s - \sin(\beta_r \cdot t_s)) + \left( \frac{\epsilon_{si}}{\epsilon_{ox}} \cdot t_{oxf} \cdot \beta_r \right) \cdot \frac{1}{4 \cdot \beta_r} \cdot [2 \cdot \beta_r \cdot t_s + \sin(\beta_r \cdot t_s)]$$

$$i_4 := \frac{\sin(2 \cdot \alpha_s \cdot L_{eff})}{2 \cdot \alpha_s} - \frac{\alpha_s}{\beta_r^2} \cdot \sinh(\beta_r \cdot L_{eff})$$

$$+ \left( \frac{\epsilon_{si} \cdot t_{oxf}}{2 \cdot \epsilon_{ox}} \right) \cdot [1 - \cos(2 \cdot \beta_r \cdot t_s)] \cdot \left( 1 + \frac{\alpha_s}{\beta_r} \right)^2$$

$$i_5 := \frac{\frac{\alpha_s}{\beta_r^2} \cdot \cosh(\alpha_s \cdot L_{eff}) \cdot \sinh(\beta_r \cdot L_{eff}) - \sin(\alpha_s \cdot L_{eff}) \cdot \cos(\beta_r \cdot L_{eff})}{\left( 1 + \frac{\alpha_s}{\beta_r} \right)^2}$$

$$N_{sr} := \frac{i_{Dnum3d} \cdot [1 - \cosh(\chi_{sr} \cdot W)] - \frac{\epsilon_{si}}{\epsilon_{ox}} \cdot t_{oxf} \cdot \chi_{sr} \cdot \sinh(\chi_{sr} \cdot W)}{\sinh(\chi_{sr} \cdot W) + 2 \cdot \frac{\epsilon_{si}}{\epsilon_{ox}} \cdot t_{oxf} \cdot \chi_{sr} \cdot \cosh(\chi_{sr} \cdot W) + \left( \frac{\epsilon_{si}}{\epsilon_{ox}} \cdot t_{oxf} \cdot \chi_{sr} \right)^2 \cdot \sinh(\chi_{sr} \cdot W)}$$

$$M_{sr} := \frac{N_{sr} \cdot \sinh(\chi_{sr} \cdot W)}{1 - \cosh(\chi_{sr} \cdot W)} \quad \text{and} \quad P_{sr} := \frac{N_{sr}}{1 - \cosh(\chi_{sr} \cdot W)}$$

These equations will provide the solution when the values of all the parameters are put in the equations and the result is obtained.

#### IV. THRESHOLD VOLTAGE FORMULATION

The model of the threshold voltage is presented for the FD SOI MOSFET. The front gate Threshold voltage ( $V_{TF1}$ ) of narrow width SOI MOSFET is defined as  $V_{TF1} = V_{gf}$ , when  $\varphi(0, y_{min}^f, W/2) = 2 \phi_b$ , here  $y_{min}^f$  is the position of surface potential in lateral direction. By differentiating the equation with respect to  $y$  at  $x = 0$  and  $z = W/2$ . Solving the equation, the solution came in form.

The Bisection method is used to calculate

$$y_{min}^f \cdot \frac{\partial \varphi(x, y, z)}{\partial y} \Big|_{x=0, y=y_{min}^f, z=W/2} = 0$$

On solving the equations, the calculation will be as follows,

$$V_{tf} := V_{tfo} - \Delta V_{tf1} - \Delta V_{tfw}$$

where

$$\Delta V_{tfw} := \frac{2 \cdot \epsilon_{si}}{C_{oxf}} \cdot P_{sr} \cdot \sinh\left(\frac{\chi_{sr} \cdot W}{2}\right) \cdot \frac{\sin(\alpha_s \cdot (y - L_{eff}))}{\cos(\alpha_s \cdot L_{eff})} \cdot \beta_r$$

From these equations, we can conclude that the  $V_{tfo}$  do not depend on channel length and width and hence, it is the threshold voltage of the long and narrow SOI MOSFET.  $V_{tf1}$  is varying with the effective channel length and the drain-source voltage but do not depend on channel width. This implies that the short channel effects reduce the threshold voltage. However, the narrow width effect leads to the reduction of the  $V_{tfw}$ .

#### V. RESULTS

Various results are obtained for the FDSOI MOSFET by using all the solutions of the Laplace equations i.e. the 1-D, 2-D and 3-D equations. These equations are also called as line potential, surface potential and the volume potential respectively.

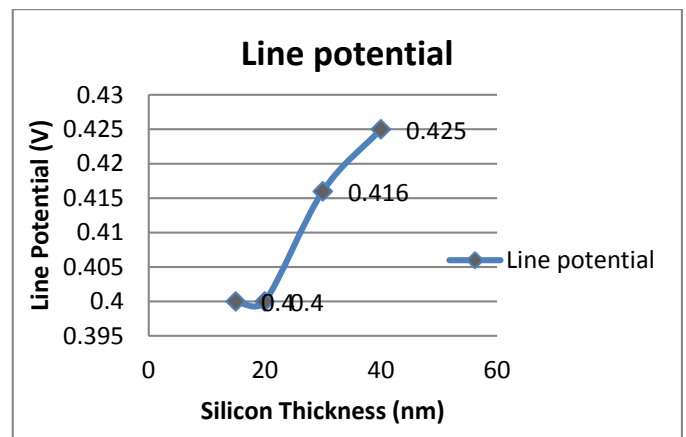
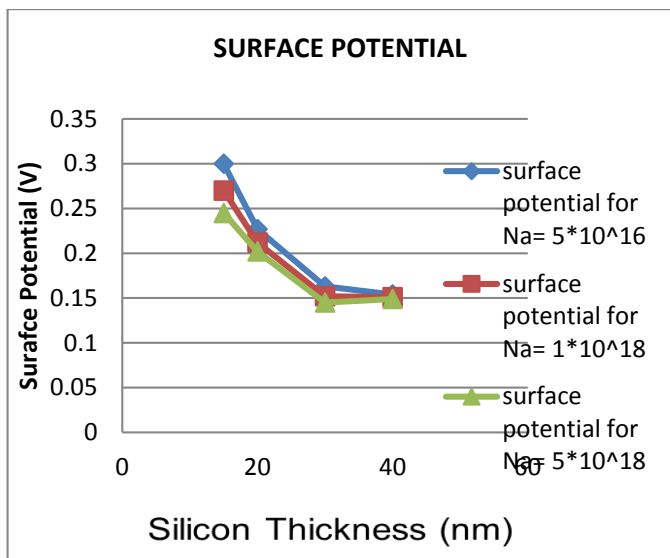


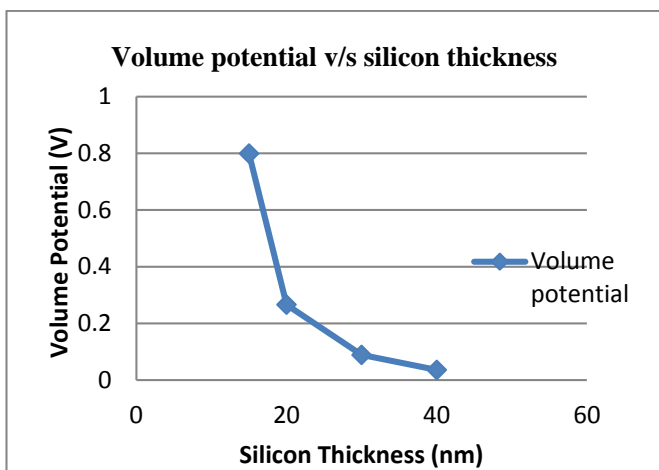
Fig 3. Variation of line potential with silicon thickness for  $x=10\text{nm}$

Figure 3, we observe that the line potential increases as the thickness of the silicon gets increased. After the variation of the line potential, surface potential is varied. When the surface potential varies for the different doping concentration as shown in figure 4 along the increasing silicon thickness, we conclude that the surface potential lowers down as the silicon thickness increases. Even the increase in the doping concentration reduces the surface potential of the device.



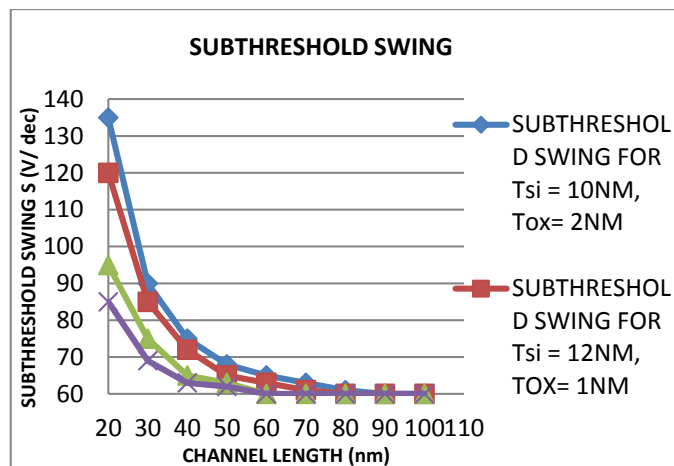
**Fig 4.** Variation of surface potential with silicon thickness for different doping concentration

Figure 5 shows the variation of the volume potential with the silicon thickness. There is decrease in the volume potential as the silicon thickness increases.



**Fig 5:** Variation of volume potential with silicon thickness

Diffusion phenomenon leads to the subthreshold drain current in the device. When gate voltage increases, the off-state leakage current increases due to the subthreshold drain current for shorter channel length. This is due to the increase of the DIBL and hence, the gate loses control over the channel with decrease in the channel length due to the increased dominance of the electrical charges of the source/drain over channel. There is increase in slope of the subthreshold current which indicated that the switching characteristics improvement with increasing gate length.



**Fig 6:** Variation of subthreshold swing with the channel length

Figure 6 represents the way of tuning a device's switching characteristics for the scaling trends. There is a drastic increase in the value of the subthreshold swing below a finite gate length. It is due to the severe increase in the short channel effects with decreasing gate length as the gate has less control over the channel. Also, the thinner channel shows less swing value, i.e. gate enhances control over the channel.

Therefore, it can be analysed that the switching characteristics of the device improves when the dimensions are properly tuned i.e. the device channel thickness and the gate oxide thickness. The characteristics deteriorate when the gate oxide thickness increases as the gate electric field intensity reduces over the channel. However, the thinner channel shows reduction in swing.

## VI. CONCLUSIONS

This paper presents the surface potential based subthreshold model and swing analysis of proposed device. An effort has been made to analyse the best operating performance model for the device in terms of surface potential, off state leakage current and switching characteristics. We have concluded that to model the structure, there has to be a balance between the various parameters of the device.

## REFERENCES

- [1]. International Technology Roadmap for Semiconductors, 2009.
- [2]. E. Suzuki, K. Ishii, S. Kanemaru, T. Maeda, T. Tsutsumi, T. Sekigawa, K. Nagai, and H. Hiroshima, —Highly suppressed short-channel effects in ultrathin SOI n-MOSFETs, *IEEE Trans. Electron Devices*, **47**(2), pp. 354–359, Feb. 2000.
- [3]. Y.-K. Choi, K. Asano, N. Lindert, V. Subramanian, T.-J. King, J. Bokor, and C. Hu, —Ultrathin-body SOI MOSFET for deep-sub-tenth micron era, *IEEE Electron Device Lett.*, **21** (5), pp. 254–255, May 2000.

- [4]. J. Pretet, S. Monfray, S. Cristoloveanu, and T. Skotnicki, —Silicon-on-nothing *MOSFETs*: performance, short-channel effects, and back gate coupling, *IEEE Trans. Electron Devices*, **51**(2), pp. 240–245, Feb. 2004.
- [5]. T. Ichimori and N. Hirashita, —Fully-depleted *SOI CMOSFETs* with the fullysilicided source/drain structure, *IEEE Trans. Electron Devices*, **49**(12), pp. 2296–2300, Dec. 2002.
- [6]. Andreas Plöchl, and Gertrud Krauter (2000) Silicon-on-Insulator: material aspects and applications. *Solid-State Electronics*, **44**, 775-782.
- [7]. Lim, H.-K. ,Fossum J.G. —Threshold voltage of thin-film Silicon-On- Insulator (SOI) MOSFETs, *IEEE Trans. on Electron Devices*, **30**(10), pp1244-1251.
- [8]. Wilk G.D., Wallace R.M. and Anthony J.M., —High-k gate dielectrics: Current status and materials properties considerations, *J. Appl. Phys.* ,**89**,pp. 5243-5275,2001.
- [9]. BSIM4.6.1 Manual. May2007.
- [10]. Thomas Skotnicki, James A.Hutchby, —The End of CMOS scaling, *IEEE Circuits & Devices*, FEB 2005.
- [11]. Q. Chen, K. A. Bowman, E. M. Harrell, , J. D. Meindl, —Double jeopardy in the nanoscale court, *IEEE Circuits Devices Mag.*, **19**( 1) pp. 28–34, Jan.2003.
- [12]. Adelmo Ortiz-Conde, Francisco J. García-Sánchez, Juan Muci, Slavica Malobabic, Jun J. Liou, "A Review of Core Compact Models for Undoped Double-Gate SOI MOSFETs, *IEEE TRANSACTIONS ON ELECTRON DEVICES*, **54**( 1), JANUARY 2007.
- [13]. Jooyoung Song, BoYu, Yu Yuan, Yuan Taur, "A Review on Compact Modeling of Multiple-Gate MOSFETs, *IEEE TRANSACTIONS ON CIRCUITS AND SYSTEMS*, **56**,( 8), AUGUST 2009.
- [14]. A. Ortiz-Conde, F. J. García-Sánchez, S. Malobabic, —Analytic solution of the channel potential in undoped symmetric dual-gate MOSFETs, *IEEE Trans. Electron Devices*, **52**(7), pp. 1669–1672, Jul. 2005.
- [15]. J. M. Sallese, F. Krummenacher, F. Pregaldiny, C. Lallement, A. Roy, and C. Enz, —A design oriented charge-based current model for symmetric DG MOSFET and its correlation with the EKV formalism, *Solid State Electron.*, **49**( 3), pp. 485–489, Mar. 2005.
- [16]. Prashant Mani, Manoj K. Pandey, —Surface Potential and Threshold Voltage Model of Fully Depleted Narrow Channel SOI MOSFET Using Analytical Solution of 3D Poisson's Equation, *JNEP*, **7**(2), pp. 2015